# Supplementary Information

## Efficient Carbon Dot-Based Phosphorescent Materials with Time-Dependent Color-Changing through Surface Modification

*Xuejun Ma,[+1] Chao Li,[+2] Zhichao Zhu,[1] Xiaofan Xia,[1] Yanhao Hu,[1] Usman Hamid,[3] Junhua Hu,[1] Jinyang Zhu,[*1] and Jinhao Zang[*3]*

1. X. Ma, Z. Zhu, X. Xia, Y. Hu, J. Hu, J. Zhu

State Centre for International Cooperation on Designer Low-Carbon & Environmental Materials, School of Materials Science and Engineering, Zhengzhou University, Zhengzhou 450001, P.R. China

2. C. Li

Zhongyuan Critical Metals Laboratory Zhengzhou University Zhengzhou 450001, P. R. China

3. U. Hamid, J. Zang

Key Laboratory of Material Physics, Ministry of Education, School of Physics, Zhengzhou University, Zhengzhou 450052, P.R. China

Email: zhujinyang1127@zzu.edu.cn (J. Zhu), abner_zang@163.com (J. Zang)

## Supporting Figures

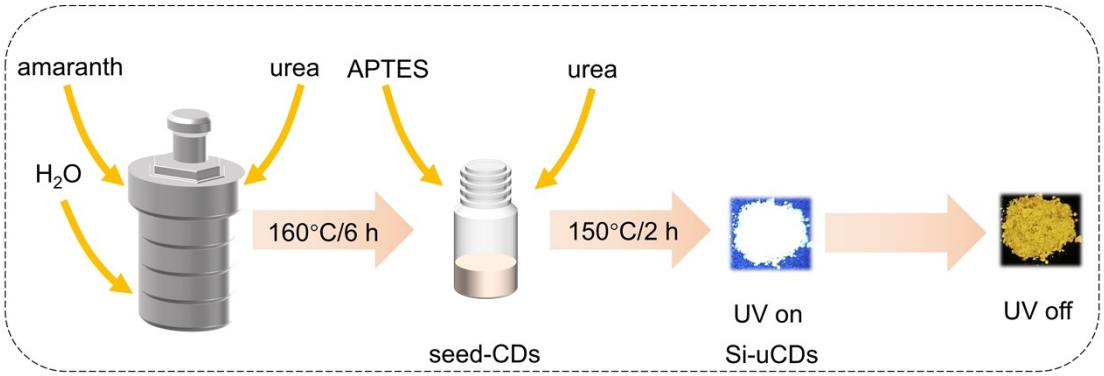


**Fig. S1** Schematic diagram of the synthesis of Si-uCDs.

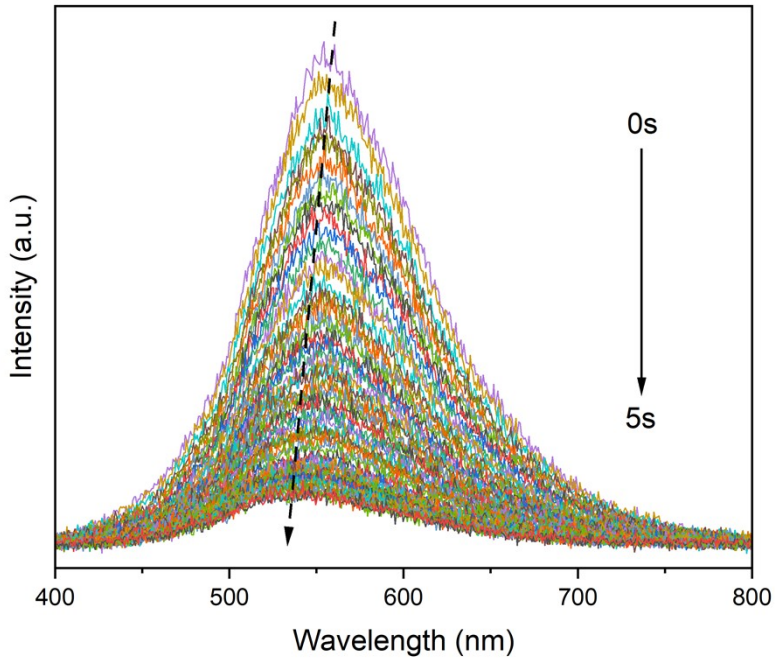


**Fig. S2** RTP emission spectra of Si-uCDs at different delay times, excited with 365 nm UV lamp.

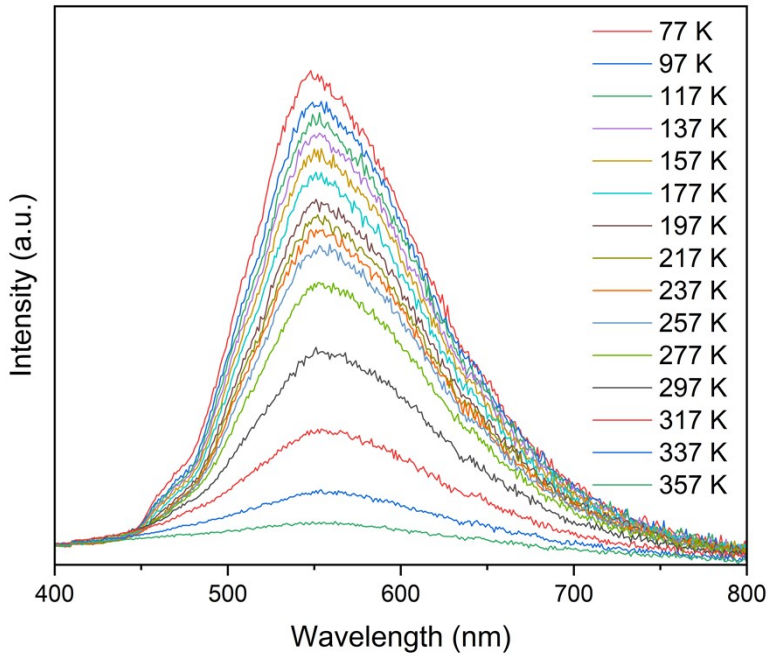


**Fig. S3** Afterglow emission spectra of Si-uCDs excited by 365 nm UV light from 77 K to 357 K.

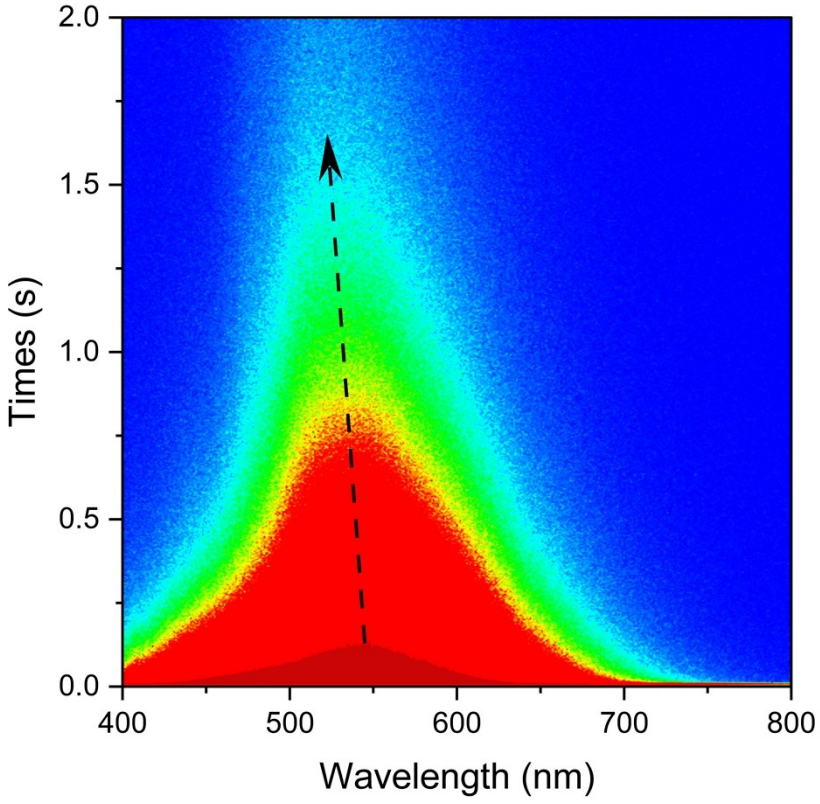


**Fig. S4** Time-resolved emission mapping of the afterglow of Si-uCDs under 365 nm excitation.

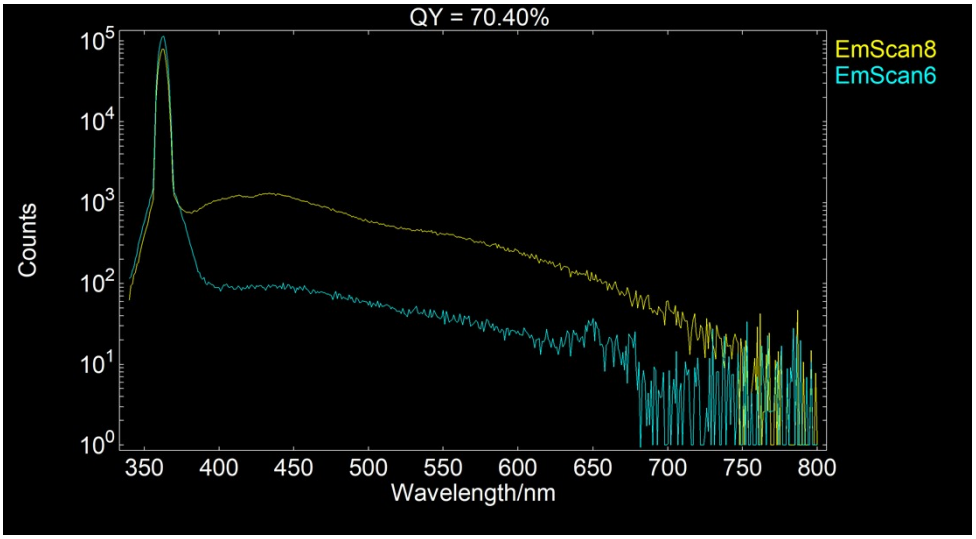


**Fig. S5** PL QY of Si-uCDs powder under the excitation at 365 nm.

The PL QY was measured at room temperature using a PL QY measurement system FS5 installed with a commercial integrating sphere from Edinburgh Instruments. The PL QY ($\Phi$) is given by the following formula:

$$\Phi = \frac{N_{em}}{N_{abs}} = \frac{\int \frac{\lambda}{hc}[I_{em}^{sample}(\lambda) - I^{reference}_{em}(\lambda)]d\lambda}{\int \frac{\lambda}{hc}[I_{ex}^{sample}(\lambda) - I^{reference}_{ex}(\lambda)]d\lambda}$$

where $N_{em}$ and $N_{abs}$ are the number of photons absorbed and emitted by a sample, respectively; $h$ is the Planck's constant; $c$ is the velocity of light; $I_{em}^{sample}$ and $I^{reference}_{em}$ are the emission intensities measured with and without a sample, respectively; $I_{ex}^{sample}$ and $I^{reference}_{ex}$ are the intensities of the excitation radiation measured with and without a sample, respectively.

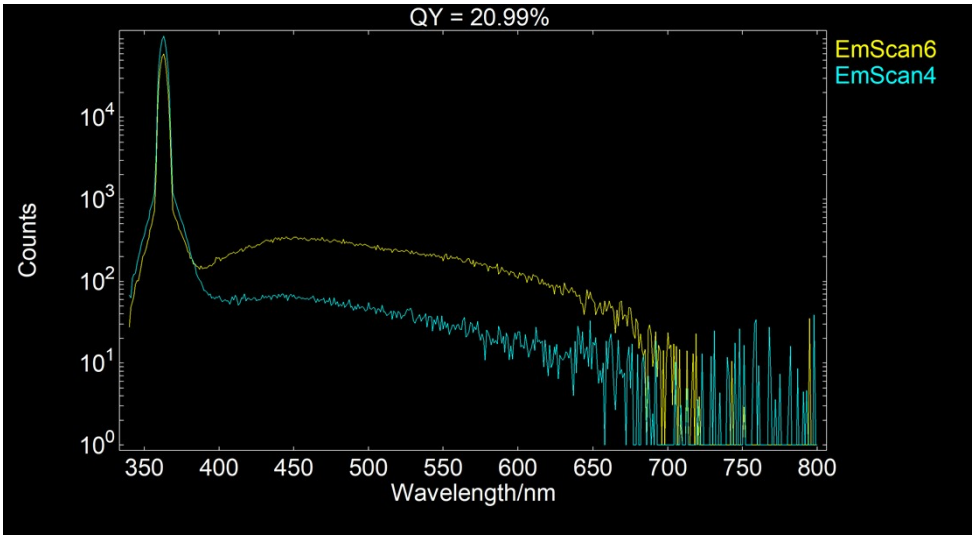


**Fig. S6** PL QY of uCDs powder under the excitation at 365 nm.

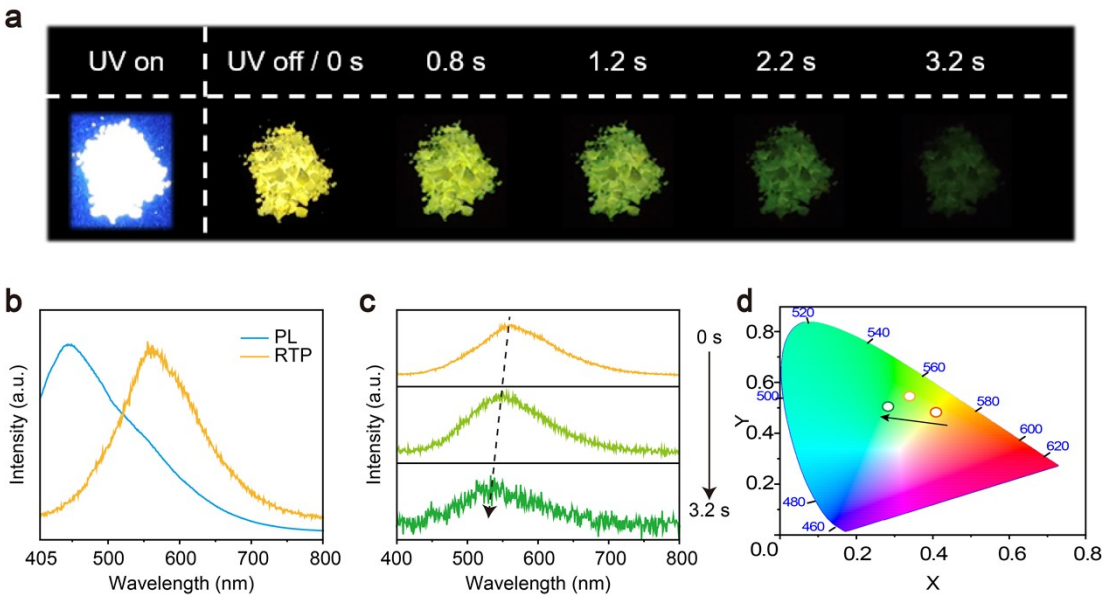


**Fig. S7** (a) Images of uCDs powder, taken before and after excitation using a 365 nm UV lamp. (b) PL and RTP emission spectra of uCDs powder under the excitation at 365 nm. (c) RTP emission spectra of uCDs at different delay times, excited with 365 nm UV lamp. (d) The CIE chromaticity diagram showing the coordinates of the uCDs presented in (c).

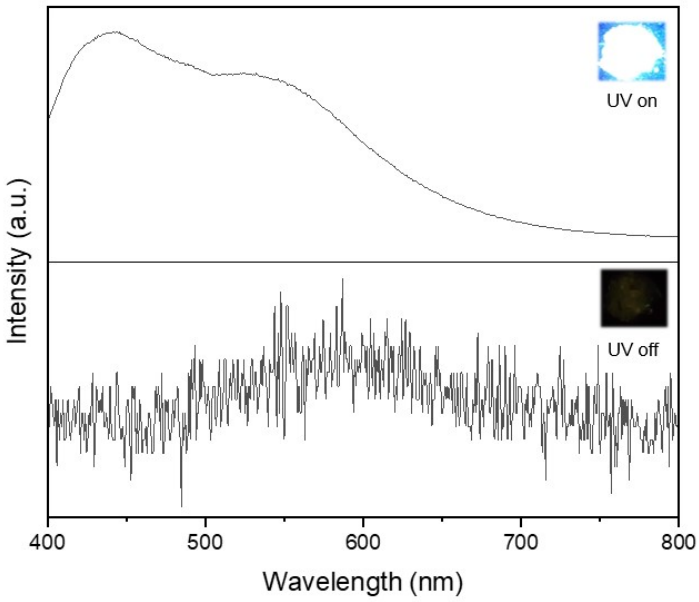


**Fig. S8** PL and afterglow emission spectra of Si-CDs powder with the 365 nm excitation source under ambient conditions.

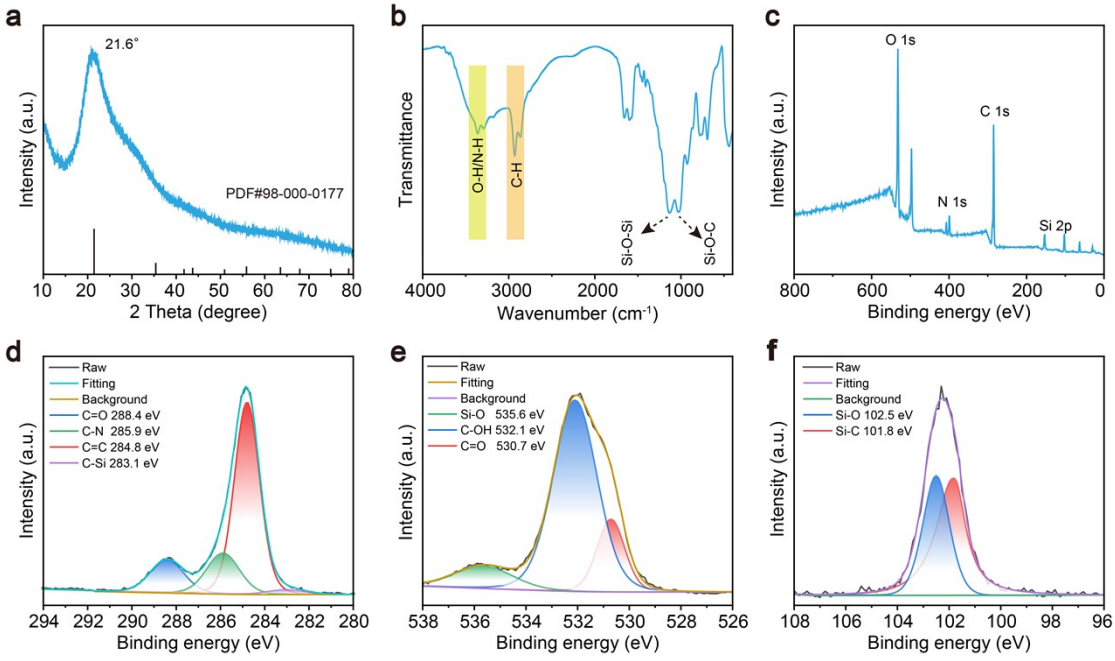


**Fig. S9** (a-f) XRD pattern (a), FT-IR spectrum (b), and XPS survey spectrum (c) High-resolution XPS spectrum and corresponding fitting results for C 1s (d), O 1s (e) and Si 2p (f) of Si-CDs.

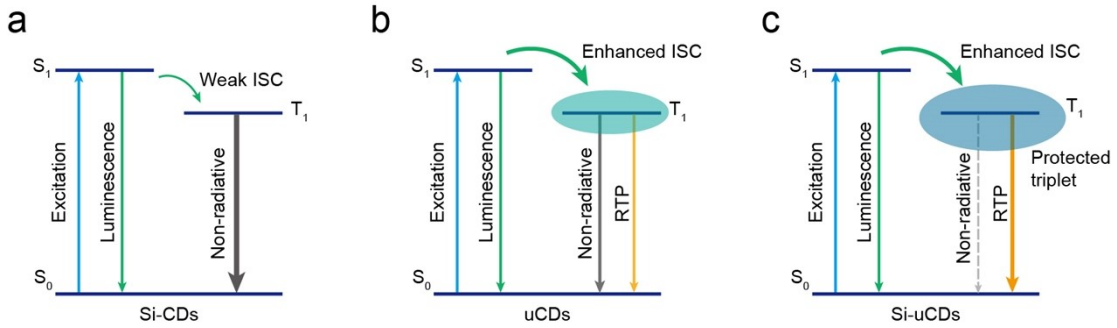


**Fig. S10** Proposed RTP emission mechanism for Si-CDs, uCDs and Si-uCDs.

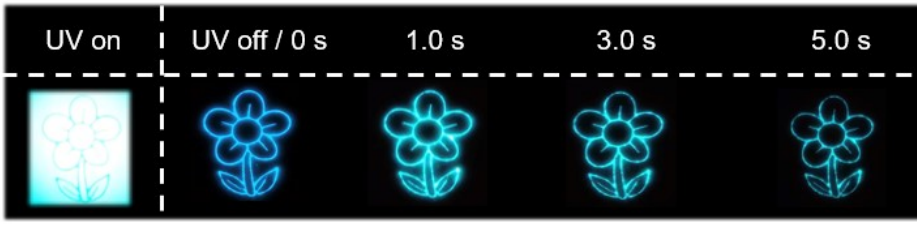


**Fig. S11** Applications of conventional afterglow materials in anti-counterfeiting technology.

**Table S1.** Afterglow lifetimes of Si-uCDs at 545 nm, 555nm and 565 nm.

| Ex. (nm) | Em. (nm) | $\tau_1$ (ms) | $A_1$ (%) | $\tau_2$ (ms) | $A_2$ (%) | $\tau_3$ (ms) | $A_3$ (%) | $\tau_{ave}$ (ms) |
|---|---|---|---|---|---|---|---|---|
| 365 | 545 | 60.38 | 17.46 | 246.31 | 56.34 | 879.12 | 26.20 | 379.64 |
| 365 | 555 | 23.52 | 17.90 | 204.89 | 57.18 | 828.56 | 24.91 | 327.80 |
| 365 | 565 | 16.62 | 11.77 | 155.12 | 55.48 | 631.01 | 32.75 | 294.68 |

**Table S2.** Atomic percentage in Si-CDs, u-CDs and Si-uCDs.

| Sample | C | N | O | Si |
|---|---|---|---|---|
| Si-CDs | 1 | 0.17 | 0.62 | 0.15 |
| u-CDs | 1 | 0.98 | 0.78 | 0 |
| Si-uCDs | 1 | 0.61 | 0.70 | 0.17 |

The atomic percentages of the samples are shown in the Table S2, no Si element was detected in uCDs, confirming the absence of APTES modification. Both uCDs and Si-uCDs exhibited higher N content than Si-CDs, attributable to urea acting as N source

that introduces abundant N-containing functional groups. Notably, both Si-CDs and Si-uCDs exhibit high Si content, confirming the formation of an extensive covalent Si-O network within the system, which can effectively suppress non-radiative decay of triplet excitons.